

Melt Rheology of Some Model Comb Polystyrenes[†]

J. Roovers* and W. W. Graessley*

National Research Council of Canada, Ottawa, Ontario K1A 0R9, Canada, and Department of Chemical Engineering and the Department of Materials Science, Northwestern University, Evanston, Illinois 60201. Received October 22, 1980

ABSTRACT: This rheological study was performed on two series of narrow molecular weight distribution comb polystyrenes. The two series were built from backbones with $M_{bb} = 275\,000$ and $M_{bb} = 860\,000$, respectively. All combs have about 30 branches increasing from $M_{br} = 6500$ to $M_{br} = 98\,000$ through the series. The zero-shear viscosities of 0.255 g/mL solutions of the combs were correlated with their Θ -temperature intrinsic viscosity, $[\eta]_{\Theta}$. The dynamic moduli of the comb melts were measured over a wide range of frequencies and temperatures by the eccentric rotating disk method. The zero-shear viscosities of the comb polystyrenes are less than those of linear polystyrenes of the same molecular weight but larger when the comparison is made at constant $[\eta]_{\Theta}$. The observed enhancement can be correlated with the average end-to-end molecular weight, \bar{M}_{EE} , of the comb. The zero-shear recoverable compliance of the combs at hand can be described by a model in which the linear backbone is diluted by the material in the branches. Accordingly, for the combs $J_{eR} = J_e^{\circ}(c_{bb}RT/M_{bb}) = 0.4(c_{bb}M_{bb}/\rho M_c')^b$, where $b = 0$ when $c_{bb}M_{bb} < \rho M_c'$ and $b = -1$ when $c_{bb}M_{bb} > \rho M_c'$. The plateau modulus G_N° appears to be the same for linear, star, and comb polystyrenes. The frequency dependence of the dynamic moduli revealed three relaxation mechanisms. The low-frequency (long time) relaxation was identified with movement of the whole molecule, the relaxation at intermediate times is related to movement of the branches, and the high-frequency relaxation is identical with that found in the transition zone of linear and star polystyrenes.

Introduction

Many commercial polymers contain long-chain branched molecules which strongly influence their processability.¹ Model star polymers have been studied extensively in an effort to elucidate the effect of branching on the rheological properties of branched polymers.²⁻⁹ Some knowledge about the rheological properties of comb polymers seems desirable in order to bridge the "structure gap" between randomly branched commercial polymers and the model stars.

Studies of the melt zero-shear viscosity (η_0) of flexible linear polymers have now well established two regions.^{2,10} At low molecular weight η_0 depends linearly on the molecular weight (M); at high molecular weight η_0 depends on $M^{3.4}$. The two regions are separated by a characteristic molecular weight M_c . Low molecular weight polymers move independently, but the movements of high molecular weight polymers are retarded by entanglements. Similarly, the zero-shear recoverable compliance (J_e°) is directly proportional to M at low molecular weight, but is independent of M at high molecular weight. The two regions are separated by another characteristic molecular weight M_c' . These characteristics are consistent with the idea that reptation is an important mode of configurational relaxation in highly entangled linear chains.¹¹

Some progress has recently been made in the elucidation of the melt rheology of star polymers. For low molecular weight melts and in dilute solution, η_0 and J_e° are found to be lower than in linear polymers of the same molecular weight.²⁻⁹ In fact, the experimental results agree with theoretical predictions^{2,12} that η_0 for linear and star polymers is the same at identical unperturbed radius of gyration ($\langle S^2 \rangle_0$). Also, the lower J_e° values observed in low molecular weight stars agree with decreases calculated from the Rouse-Ham theory.¹³

High molecular weight stars have values of η_0 many times higher than predicted from considerations of size alone, often exceeding those of linear polymers of the same molecular weight.^{3,4,8,9} This enhancement in η_0 increases exponentially with the number of entanglements per

branch.^{2,8} High molecular weight stars also have higher J_e° values than linear polymers.^{5,8,9} The values, however, remain in surprisingly good agreement with the Rouse-Ham prediction.^{8,9} These observations are consistent with the idea that the presence of long branches suppresses reptative motions^{8,14} and that configurational reorganization then proceeds more slowly, perhaps by the random jumping processes similar to those of the Rouse model.

It would be of obvious interest to test the principles established for stars on comb polymers. Extensive studies of the rheological properties of comb polystyrenes were performed by Nagasawa and co-workers.¹⁵⁻¹⁷ The zero-shear melt viscosities of their combs were always lower than those of linear polymers of the same molecular weight.^{15,17} Pannell showed, however, that these η_0 data and his own results show enhancement when compared at constant calculated $\langle S^2 \rangle_0$.¹⁸ The meaning of this comparison is uncertain, however, because the combs have larger unperturbed dimensions than calculated from the random-flight assumption.^{16,19,20} Poly(vinyl acetate) combs have higher melt viscosities than the linear polymers.²¹ The enhancement was found to depend exponentially on the branch length.² Enhanced zero-shear viscosities have also been reported for solutions of randomly branched poly(vinyl acetates).²²

Reported J_e° data for melts of polystyrene combs vary between 3×10^{-6} and 1×10^{-5} cm²/dyn;^{15,17} i.e., they are always higher than the maximum value for high molecular weight linear polystyrenes (1.2×10^{-6} cm²/dyn).¹⁰

From these studies no clear understanding of the factors affecting η_0 and J_e° in combs has evolved. The many different types of combs present problems, as do large heterogeneity in the samples²¹ and dilution of the combs by linear material.¹⁸ New rheological data on polystyrene combs, both on their concentrated solutions and on the melts, are presented here, and an interpretation of these and some older results is attempted.

Experimental Section

The synthesis and characterization of the C6 and C7 combs have been described.²⁰ The data pertinent to the rheological work are given in Table I. The backbone and branches were narrow molecular weight distribution anionically prepared polystyrenes. The C6 polymers all have a backbone molecular weight $M_{bb} = 275\,000$ and approximately $p = 30$ branches. Branch molecular

* Address correspondence to J.R. at NRCC and to W.W.G. at Northwestern University.

[†] Issued as NRCC No. 19185.

Table I
Characteristics and Dilute-Solution Properties of
Comb Polystyrenes

sample	$M_w \times 10^{-5}$	$M_{nbr} \times 10^{-3}$	p^a	g_{th} (eq 7)	g_{∞}^b	$[\eta]_0$, dL/g
C6bb	2.75					0.414
C612	4.75	6.5	31	0.597	0.729	0.377
C622	6.24	11.7	30	0.473	0.588	0.382
C632	9.13	25.7	25	0.353	0.472	0.389
C642	16.3	47.0	29	0.241	0.338	0.413
C652	31.3	98.0	29	0.175	0.267	0.489
C7bb	8.6					0.776
C712	10.55	6.5	30	0.819	0.886	0.753
C722	11.9	11.7	28	0.732	0.825	0.718
C732	15.3	25.7	26	0.583	0.669	0.700
C742	22.3	47.0	29	0.426	0.538	0.694
C752	36.2	98.0	28	0.300	0.429	0.721

^a Average number of branches per molecule. ^b Reference 20.

weights, M_{br} , increase from 6500 to 98 000 through the series. The C7 series differs only in $M_{bb} = 860\,000$, while p and M_{br} are the same as in the C6 series. From all available evidence, the molecular weight distribution and the variation of comb structure in each sample are minimum for a random coupling process.²⁰ The resulting M_w/M_n of the combs is less than 1.06.²⁰ The combs have no measurable θ -temperature depression in cyclohexane.²⁰ Their glass transition temperatures are indistinguishable from those of high molecular weight linear polystyrene.²⁰

Viscosity measurements on 0.255 g/mL solutions in *n*-butylbenzene ($d = 0.8524$, $\eta = 9.5 \times 10^{-3}$ P) of the C6 combs were made at 24.2 °C in calibrated Cannon-Ubbelohde viscometers.^{6,7} All flow times were longer than 500 s. The maximum shear rate was in all cases less than 2 s^{-1} , which is well within the Newtonian region (see C65 in Figure 1). Measurements of 0.255 g/mL solutions of the C7 combs at 24.2 °C were performed with a cone-plate geometry on a Rheometrics mechanical spectrometer. The radius was 2.5 cm and the gap angle was 0.1 rad. The first normal stress difference ($p_{11} - p_{22}$) was used to calculate the zero-shear recoverable compliance²³

$$J_e^0 = \frac{1}{2} \lim_{\dot{\gamma} \rightarrow 0} \frac{p_{11} - p_{22}}{\eta^2 \dot{\gamma}^2} \quad (1)$$

Dynamic moduli on melts of the linear backbones and the combs were obtained with the Rheometrics mechanical spectrometer in the eccentric rotating disk (ERD) mode. The steady-state storage modulus (G') and the loss modulus (G'') were obtained as functions of the frequency (ω) from measurements of steady forces.²⁴ The platen radius was 1.25 cm and the platen separation varied between 0.100 and 0.120 cm. The viscoelastic measurements were performed in the linear regime by using a small eccentricity and reducing it at high frequencies as described earlier.⁹ The instrumental compliance correction ($K = 3.44 \times 10^{-9}$ cm/dyn) was applied to evaluate the correct eccentricity.²⁴ A 10% uncertainty in this constant would only slightly affect the moduli.

The polystyrene powders were mixed with 0.02% Santonox and vacuum molded into clear disks. Disks of C622 and C632 were very brittle at room temperature.¹⁷ Rheological measurements were made between 140 and 210 °C. The highest temperature used depended on the need to penetrate the limiting region ($G'' \propto \omega$, $G' \propto \omega^2$) at the lowest available frequency. Degradation of the polymers became a problem above 190 °C despite continuous flushing of the sample compartment with high-purity nitrogen. Measurements over short periods (2 h) and the use of many test disks provided reproducibility to within 5% at high temperatures.

Results

The steady shear rate data obtained on 25.5% solutions of the C7 combs are plotted in Figures 1 and 2. The viscosity and $(p_{11} - p_{22})/(\eta \dot{\gamma})^2$ become independent of shear rate ($\dot{\gamma}$) at low shear rates. The zero-shear data are collected in Table II. The zero-shear viscosities of the combs do not differ much from those of their parent backbone.

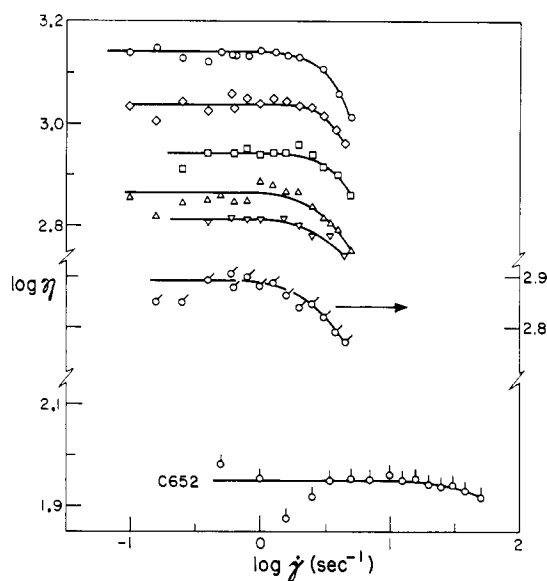


Figure 1. Shear rate dependence of viscosities for 0.255 g/mL solutions of comb polystyrenes. From top to bottom, C7bb, C712, C722, C732, C742, C752, and C652.

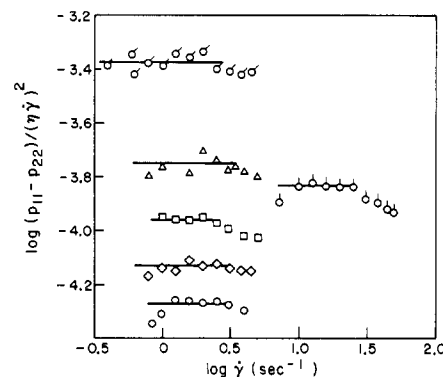


Figure 2. Normal stress data for 0.255 g/mL solutions of comb polystyrenes. Symbols as in Figure 1. Notice the different order of limiting values within the C7 series.

Table II
Zero-Shear Data for 0.255 g/mL
Solutions of Combs at 24.2 °C

sample	η_0 , P	$\eta_0/[\eta]_0^{6,6} \times 10^{-4}$	$J_e^0 \times 10^5$, cm ² /dyn
C6bb	30.0	1.01	
C612	17.0	1.06	
C622	15.5	0.89	
C632	17.9	0.91	
C642	29.4	1.01	
C652	96.1 ^a	1.08	7.4
C7bb	1390	0.74	2.7
C712	1093	0.71	3.7
C722	875	0.78	5.5
C732	725	0.76	9.0
C742	650	0.72	
C752	780	0.68	21.2

^a 89.0 P obtained with the cone-plate geometry.

They go through a shallow minimum with increasing branch length. The zero-shear recoverable compliance increases steadily with increasing branch length.

Typical storage and loss moduli-frequency curves obtained on the melts of the combs are shown in Figures 3 and 4. These master curves at 169.5 °C are composed of data obtained at different temperatures and shifted along the frequency axis. The experimental shift factors (a_T) of

Table III
Melt Characteristics of Combs at 169.5 °C

sample	$\eta_0 \times 10^{-6}$, P	$J_e^\circ \times 10^6$, cm ² /dyn	$G_N^\circ \times 10^{-6}$, dyn/cm ²	Γ^a	g_2^b	g_{2th}^c
C6bb	3.1	1.2	2.05		0.41	1.0
C612	2.8	3.5	2.0	1.4	0.66	0.94
C622	2.7	5.4	2.3	1.8	0.78	0.88
C632	3.0	11.5	2.1	1.8	1.14	0.71
C642	5.4	21.5	2.1	2.3	1.19	0.52
C652	34.9	33.0	2.2	4.6	0.95	0.30
C7bb	145	1.25	2.1		0.13	1.00
C722	450	2.75	1.95	4.6	0.21	0.98
C732	570	5.8	1.95	7.0	0.34	0.93
C742	>650	~16		(8.4)	(0.65)	0.83

^a Equation 6. ^b Equation 11. ^c Reference 28.

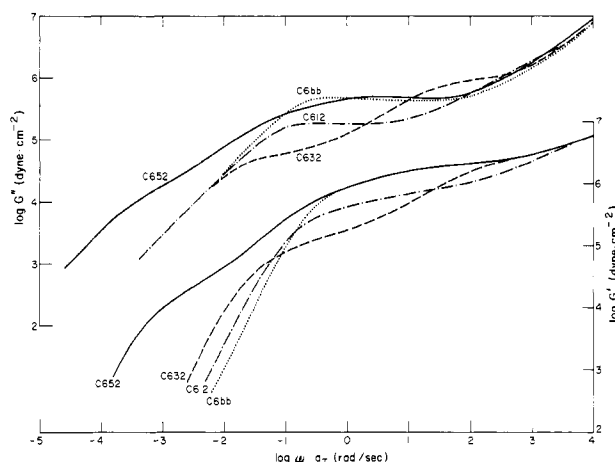


Figure 3. Dynamic moduli-frequency master curves for melts of the C6 combs. Reference temperature is 169.5 °C. Numerical data on all samples are available on request from the authors or from CISTI, NRCC, Ottawa, Ontario, Canada.

the combs were the same as for linear and star polystyrene melts.^{9,15,17} From Figures 3 and 4 it can be seen that the combs have an extended plateau region characteristic of entangled polymers. While the low-frequency loss moduli (and thus the viscosities) do not change much in going from C6bb to C632, the low-frequency storage moduli increase progressively with branch length. Figures 3 and 4 also show that departures from limiting behavior occur at lower frequency for the combs than for linear polymers with comparable viscosity.

The dynamic moduli-frequency curves of the combs (Figures 3 and 4) show two inflections in the plateau-terminal region, suggesting two distinct relaxation processes. The location of these inflections depends on both the backbone and branch molecular weights. The behavior of C642 is shown in Figure 5. Here also the inflections are distinguishable and well separated from the transition region. This behavior will be discussed in a later section. Note also the "Rouse-like" character of G' and G'' at intermediate frequencies: the moduli change fairly abruptly from limiting behavior $G' \propto \omega^2$ and $G'' \propto \omega$ to $G' \propto \omega^{1/2}$ and $G'' \propto \omega^{1/2}$.

Values of zero-shear viscosity and recoverable compliance were derived from²³

$$\eta_0 = \lim_{\omega \rightarrow 0} \frac{G''(\omega)}{\omega} \quad (2)$$

and

$$J_e^\circ = \frac{1}{\eta_0^2} \lim_{\omega \rightarrow 0} \frac{G'(\omega)}{\omega^2} \quad (3)$$

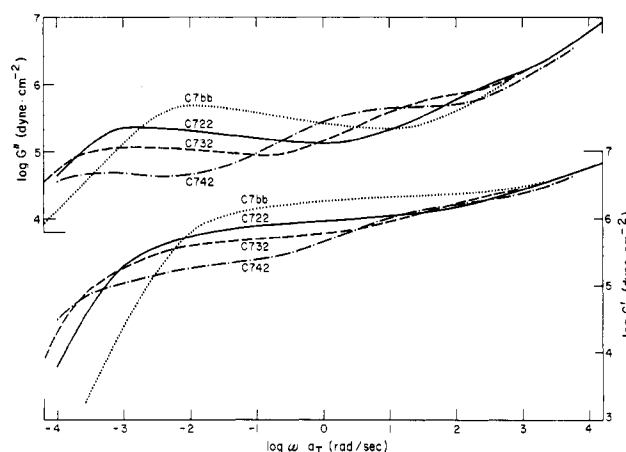


Figure 4. Dynamic moduli-frequency master curves for C7 series combs. Reference temperature is 169.5 °C.

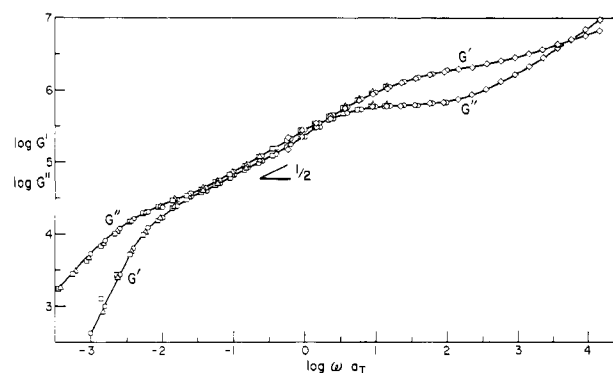


Figure 5. Dynamic moduli-frequency master curves for C642 at 169.5 °C. Symbols for different measurement temperatures: (□) 190.4; (Δ) 180.0; (○) 169.5; (◇) 140.7 °C.

The data are collected in Table III. The values for C742, for which the limiting behavior was not quite attained, were estimated by superposing on the terminal region of C732. This superposition required both a vertical and a horizontal shift, so the results may be somewhat in error.

The plateau moduli for the combs were estimated from²³

$$G_N^\circ = \frac{2}{\pi} \int_{-\infty}^{+\infty} [G''(\omega) - G_s''(\omega)] d \ln \omega \quad (4)$$

where the contribution from the transition region, $G_s''(\omega)$ ($\omega > 1 \text{ s}^{-1}$ at 169.5 °C), was obtained from the data on linear polystyrene⁹ as shown by the example of C632 in Figure 6. Corrections for the transition region contributions are most important for combs with a high weight fraction of small branches. The values of G_N° are given in Table III.

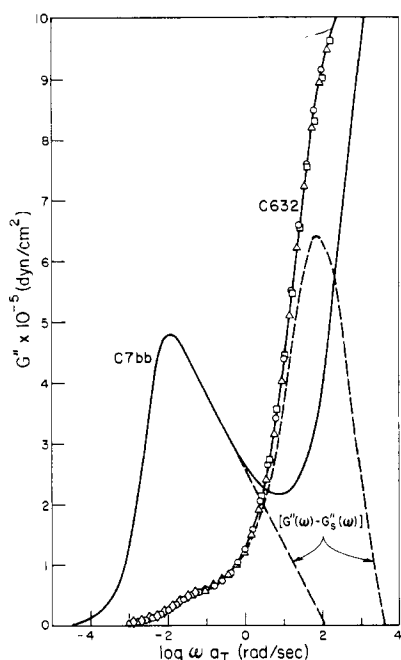


Figure 6. Loss moduli vs. $\log \omega$ used to determine the plateau modulus G_N° according to eq 4. Measurement temperatures: (\diamond) 190.4; (\circ) 169.5; (Δ) 150.2; (\square) 140.7 °C.

Discussion

A. Temperature Frequency Shift Factor a_T . At the outset it is useful to make a comment on the observation made here and elsewhere^{15,17} that the shift factors of the comb polystyrenes are not different from those of linear polystyrene. These shift factors have been determined mostly by superposition of moduli-frequency curves at intermediate frequencies. Only for C6 combs with small branches are low-frequency shift factors available. They do agree with those of linear polystyrene and there is no evidence to suggest otherwise for samples with longer branches. However, data for samples with the longest branches do not cover the terminal region with sufficient thoroughness to answer conclusively the question whether branched polystyrenes with enhanced zero-shear viscosities have the same temperature coefficient of viscosity as the linear polymers. A similar situation was also encountered in polystyrene stars.^{5,9}

B. Zero-Shear Viscosity. Zero-shear viscosities of stars have been correlated with η_0 of linear polymers by means of the relations^{2,7-9}

$$\eta_0 = K \langle S^2 \rangle_0^\alpha = K' [\eta]_\theta^2 \quad (5)$$

with $\alpha = 1$ or 3.4 when $\langle S^2 \rangle_0$ is either smaller or larger than that of M_e . Enhancement of η_0 is defined by²

$$\Gamma = (\eta_0)_{\text{obsd}} / (\eta_0)_{\text{calcd}} \quad (6)$$

in which Γ is the enhancement factor and $(\eta_0)_{\text{calcd}}$ is obtained from eq 5.

For combs no equivalent to eq 5, correcting for the molecular size difference, has been established. Only the size effect should be operating in 25.5% solutions. However, contrary to the results on star,^{2,5-9} plots of η_0 for the solutions vs. λM , $g_{\text{th}} M$, or $g_\theta M$ always result in lower viscosities for the combs than the corresponding linear polymers, λ being the weight fraction of backbone in the comb and g_{th} being calculated from²⁵

$$g_{\text{th}} = (\langle S^2 \rangle_{0,\text{comb}} / \langle S^2 \rangle_{0,\text{lin}})_M = \lambda + \frac{3}{p}(1 - \lambda) + \frac{(1 - \lambda)^3}{p^2} \quad (7)$$

From Table I it can be seen that for the combs²⁰

$$g_\theta = (\langle S^2 \rangle_{\theta,\text{comb}} / \langle S^2 \rangle_{\theta,\text{lin}})_M > g_{\text{th}} \quad (8)$$

Only comparison on the basis of $[\eta]_\theta$ makes the 25.5% solution data for combs and linear polymers coincide. For linear polystyrene melts $\eta_0 \propto [\eta]_\theta^{6.61}$, and $\eta_0 / [\eta]_\theta^{6.6}$ is practically a constant within each of the comb series (Table II). In particular the use of $[\eta]_\theta$ accommodates the decrease of η_0 for combs with small branches from η_0 of the parent backbone. The very low η_0 found for some other polystyrene combs with many small branches¹⁵ may well correlate with $[\eta]_\theta$. Such combs are known to have lower θ temperatures²⁷ and $[\eta]_\theta$ substantially less than values measured at the θ temperature of the linear polymer. The slightly different values for $\eta_0 / [\eta]_\theta^{6.6}$ of the C6 and C7 combs in Table II are probably due to slightly different exponents in the $\eta_0 - [\eta]_\theta$ curves for the two regions of $[\eta]_\theta$. Indeed, since M_e for 0.255 g/mL solutions of polystyrene is $(1.5 - 1.9) \times 10^5$, the exponent for the C6 combs may be somewhat lower than 6.6.

We can now compare the melt zero-shear viscosities of the combs with those of linear polystyrene at identical $[\eta]_\theta$. The zero-shear viscosity enhancements of eq 6 with $(\eta_0)_{\text{calcd}} = 8.62 \times 10^8 [\eta]_\theta^{6.61}$ are given in Table III. In all the comb melts some enhancement in η_0 is observed, and we will assume that this is due only to the same effects responsible for enhancement in stars. In particular, it is not necessary to invoke a change in the entanglement spacing of branched molecules. This point is confirmed by inspection of G_N° in Table III. Thus²³

$$M_e = \rho RT / G_N^\circ \quad (9)$$

where M_e is the molecular weight between entanglements and ρ the melt density. Within experimental precision G_N° and, therefore, M_e of the combs and linear polymers are the same ($M_e = 18000$). A similar conclusion was drawn from data on stars.^{5,9} The results obtained on the combs are more significant because the branch point density is higher, and thus any changes associated with crowding at the branch points would be more pronounced.

The viscosity enhancement of the combs is not merely limited to branch lengths greater than M_e , nor is the enhancement identical for C6 and C7 combs at the same branch length. As shown in Figure 7, Nagasawa's melt viscosities also show evidence of enhancement. Pannell's combs¹⁸ have similar enhancements when compared at $[\eta]_\theta$.

In stars the enhancement is assumed to reflect the time required for an arm to rearrange its configuration. The friction coefficient associated with arm rearrangement is predicted to increase exponentially with arm length,¹⁴ which is consistent with the exponential form of Γ in stars. It is, however, not at all clear how to extend this idea to molecules with many branch points such as the combs. We have been able to unify the observations somewhat by correlating Γ with the average end-to-end molecular weight \bar{M}_{EE} . For combs (see Appendix)

$$\bar{M}_{EE} = \frac{2p}{p+2} M_{\text{br}} + \frac{p+3}{3(p+1)} M_{\text{bb}} \quad (10)$$

which was obtained by considering the case of a regular comb with p equidistant branches. This is probably a sufficiently good approximation for combs with randomly placed branches.²⁵

The observed viscosity enhancements of the melts are plotted against \bar{M}_{EE} / M_e in Figure 8. The results for the two series of combs combine satisfactorily into a single line and the exponential dependence of Γ is retained. The same line represents Nagasawa's combs well at low

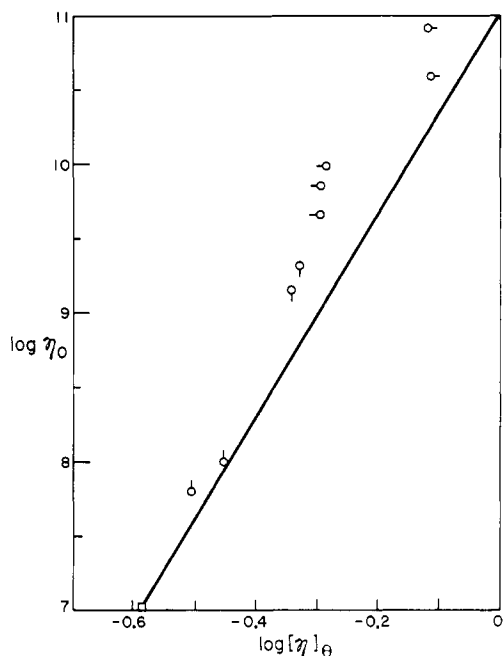


Figure 7. Melt viscosities for comb polystyrenes measured by Nagasawa et al.¹⁵ plotted against the Θ -temperature intrinsic viscosity, estimated from data given in ref 16. The line is for linear polystyrene. Symbols: (□) linear backbone polymer; (○) F series; (◐) H series; (◑) I series; (◒) J series.

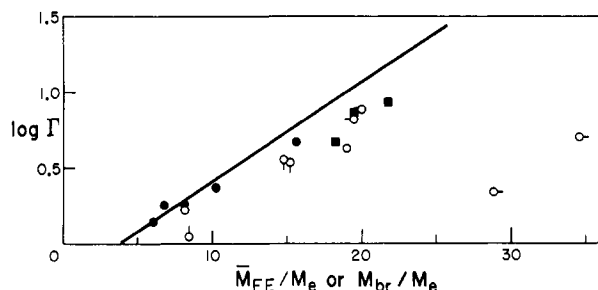


Figure 8. Viscosity enhancement factors vs. the number of entanglements per average end-to-end strand for combs (\bar{M}_{EE}/M_e). Symbols: (○) C6 series; (◐) C7 combs. Other symbols as in Figure 7. The line represents enhancements in four-arm stars as a function of \bar{M}_{br}/M_e .⁹

\bar{M}_{EE}/M_e , but deviations occur at higher values. Whether the deviations result from a failure of the model is unclear, however, as there must have been extreme experimental difficulties with such combs. Pannell's comb polystyrene data¹⁸ show large scatter but do not contradict the present results. The melt viscosities of poly(vinyl acetate) combs,²¹ all of which have $\bar{M}_{EE}/M_e > 50$, do not fit the present model however.

The line drawn in Figure 8 is taken directly from Figure 7 of ref 9 and represents the enhancements observed in four-arm star polystyrene melts. The abscissa in this case is simply M_{br}/M_e . A comparison of three- and four-arm polybutadiene enhancement factors⁸ suggests that the line for three-arm polystyrene stars would practically coincide with the comb data. Thus enhancement in our polystyrene combs and in three-arm polystyrene stars is about the same when compared at the same values of \bar{M}_{EE} and M_{br} , respectively.

C. Zero-Shear Recoverable Compliance. The Rouse-Ham theory¹³ provides an expression for the recoverable compliance of branched polymers

$$J_e^\circ = 0.4g_2 \frac{M}{cRT} \quad (11)$$

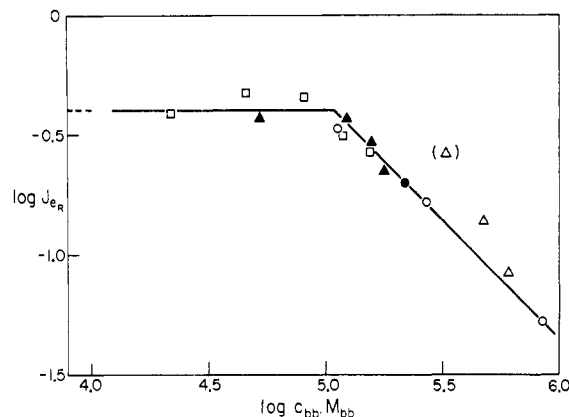


Figure 9. Reduced recoverable compliance vs. the product of the backbone concentration (g/mL) and its molecular weight. Open symbols for melts: (○) linear polymer; (◐) C6 combs; (◑) C7 combs. Full symbols for data obtained on 0.255 g/mL solutions: (●) C7bb; (▲) C7 combs.

in which c is the polymer concentration in g/mL ($c = \rho$ for undiluted polymer), $g_2 = 1$ for linear chains, and $g_2 < 1$ for branched chains, reflecting the theoretical narrowing of the relaxation time distribution produced by branching. The factor g_2 can, in principle, be calculated from the structure. An expression for g_2 in stars is available,¹³ and data on low molecular weight linear polymers and three-, four-, and six-arm stars agree well with the theory. At high molecular weights ($M > M_c' = 120\,000$ for undiluted polystyrene) J_e° for linear polymers becomes independent of M ($(J_e^\circ)_\infty \approx 1.2 \times 10^{-6}$ cm²/dyn), while J_e° for stars remains close to the theoretical values.^{8,9}

Theoretical g_2 values for regular combs with equidistant branches have become available recently.²⁸ By analogy with the small differences between g_{th} for regular and randomly branched combs, it is expected that these theoretical g_2 values will closely approximate the theoretical g_2 values for the combs at hand. The values of g_{2th} are shown in the last column of Table III.

Apparent values of g_2 , calculated from eq 11 with the experimental data, are also listed in Table III. Values of g_2 rise from the value of the parent backbone and pass through a maximum ($g_2 > 1$) with increasing branch length in the C6 series. For combs with a constant number of branch points on a high molecular weight backbone one might expect experimental J_e° values to move smoothly from that of the linear backbone, $(J_e^\circ)_\infty$, when the branches are short and values of g_2 predicted with eq 11 will initially be less than g_{2th} . This is particularly clear from a comparison of g_2 and g_{2th} in the C7 series. From observations on J_e° of star polymers,^{8,9} it is expected that g_2 calculated by eq 11 and g_{2th} approach each other when the branches of the comb become very long.

The data on J_e° can be interpreted also in another way by regarding the branches as simply serving to dilute the linear backbones. For concentrated solutions of linear polymers the compliance is given by¹⁰

$$J_e^\circ = 0.4 \frac{M}{cRT} \left(\frac{cM}{\rho M_c'} \right)^b \quad (12)$$

with $b = 0$ when $cM < \rho M_c'$ and $b = -1$ when $cM > \rho M_c'$. For the case of the backbone diluted by the branches, M in eq 12 is replaced by M_{bb} and c by $c_{bb} = \rho M_{bb}/(M_{bb} + \rho M_{br})$. The reduced compliance is then

$$J_{eR} = J_e^\circ \frac{c_{bb}RT}{M_{bb}} = 0.4 \left(\frac{c_{bb}M_{bb}}{\rho M_c'} \right)^b \quad (13)$$

Table IV
Frequency-Dependent Properties of Comb Polystyrenes at 169.5 °C

sample	ω_0, s^{-1}	$\eta_0 J_e^\circ \omega_0$	$\tau_{br},^a \text{s}$	$\tau_{bb},^a \text{s}$	$J_{br} \times 10^6,^b \text{dyn/cm}^2$	$\tau_{br},^b \text{s}$	$J_{bb} \times 10^6,^b \text{dyn/cm}^2$	$\tau_{bb},^b \text{s}$
C6bb	0.190	0.71		0.63			0.82	0.83
C612	0.065	0.63	0.0126	2.5	1.28	0.038	1.8	4.0
C622	0.04	0.58	0.063	4.0	2.3	0.114	2.5	4.4
C632	0.016	0.54	0.575	10.0	7.05	1.2	4.7	24
C642	0.0043	0.49	6.3	79	10.9	6.4	12	60
C652	0.0004	0.46	$\sim 10^3$	$\sim 10^3$	12.5	125	22	1070
C7bb	3.8×10^{-3}	0.71		22.9			0.8	39.8
C722	4.0×10^{-4}	0.50	0.01	250	0.65	0.044	1.8	245
C732	2.6×10^{-4}	0.85	0.25	630	1.38	0.21	3.3	525
C742	8.3×10^{-5}	0.85	3.9	1000	4.8	5.2	7.7	2630

^a From visual inspection of recoverable compliance vs. frequency data in Figures 10 and 11. ^b From complex analysis (eq 18).

A plot of J_{er} vs. $c_{bb}M_{bb}$ is shown in Figure 9. Both melt data and the 25.5% solution data obey eq 13, even giving the correct $M_c' \approx 1.2 \times 10^5$ for linear polystyrene.¹⁰ The combs studied by Nagasawa^{15,17} have $c_{bb}M_{bb}$ values between 10^3 and 10^4 , a range considerably below that covered here. In general, their J_{er} data are much lower than values calculated with eq 13. Only for the K402 combs, whose structure is comparable with combs of this study, do J_{er} values vary between 0.34 and 0.45. The failure of this method to correlate most of Nagasawa's comb data is probably due to the "starlike" ($M_{br} \geq M_{bb}$) structure of those combs. Equation 13 is not applicable to star molecules.

D. Frequency-Dependent Properties. As pointed out earlier, the storage and loss moduli of the combs depart from limiting behavior ($G' \propto \omega^2$ and $G'' \propto \omega$) at lower frequencies than linear polymers with the same viscosity. The onset of shear rate dependence of the steady-state viscosity is specified by a characteristic shear rate $\dot{\gamma}_0$.¹⁰ In the same way we can define ω_0 as the frequency at which the absolute value of the complex viscosity

$$|\eta^*(\omega)| = (G'(\omega)^2 + G''(\omega)^2)^{1/2} / \omega \quad (14)$$

has decreased to 0.8η . The values of ω_0 are listed in Table IV. The products $\eta_0 J_e^\circ \omega_0$, also given in Table IV, are found to be remarkably constant at 0.6 ± 0.2 , despite the large variation in structure among samples. Similar results were found for star polymers.^{8,9} The value of $\eta_0 J_e^\circ \omega_0$ is also in agreement with the value for $\eta_0 J_e^\circ \dot{\gamma}_0$, which was found to be constant for a wide variety of polymer systems.^{8,10}

The inflections in G' and G'' in the plateau-terminal region of the combs, suggesting two distinct relaxation processes, were also noted earlier. These effects appear more clearly in the components of the complex dynamic compliance, $J^*(\omega) = J'(\omega) - jJ''(\omega)$, where²³

$$J'(\omega) = \frac{G'(\omega)}{[G'(\omega)]^2 + [G''(\omega)]^2} \quad (15)$$

$$J''(\omega) = \frac{G''(\omega)}{[G'(\omega)]^2 + [G''(\omega)]^2} \quad (16)$$

Figures 10 and 11 show $J_r''(\omega) = J''(\omega) - 1/\eta_0\omega$ vs. ω for the C6 and C7 series, respectively. The high-frequency peak at $\omega = 1.6 \times 10^3 \text{ s}^{-1}$ (169.5 °C) is the same for linear, star, and comb polystyrenes of high molecular weight and is characteristic of the transition region. Two additional peaks are clearly evident for some of the combs, while there is only one low-frequency peak in the high molecular weight linear polymers. The intermediate peak, present only in the combs, nearly merges with the transition peak

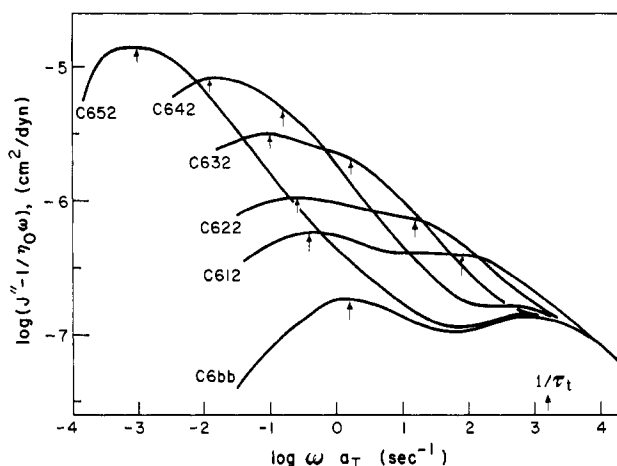


Figure 10. Recoverable loss compliance vs. frequency for melts of the C6 series at 169.5 °C. The arrows indicate the characteristic frequency estimated for each retardation mechanism.

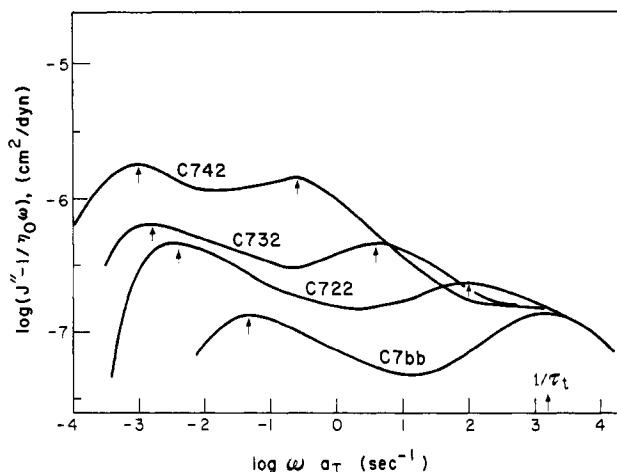


Figure 11. Same as Figure 10. Data for C7 combs.

when the branches are short but moves rapidly to lower frequencies and almost merges with the low-frequency peak in the case of C652.

The low-frequency peak of the combs moves away from that of the linear backbone to still lower frequencies. It seems reasonable to associate the intermediate dispersion with movements of the branches and the one at low frequencies with the polymer molecules as a whole.

Retardation times characterizing these dispersions, τ_{br} for the intermediate peak and τ_{bb} for the low-frequency peak, can be estimated in any of several ways. Values were calculated at the reciprocals of the peak frequency, esti-

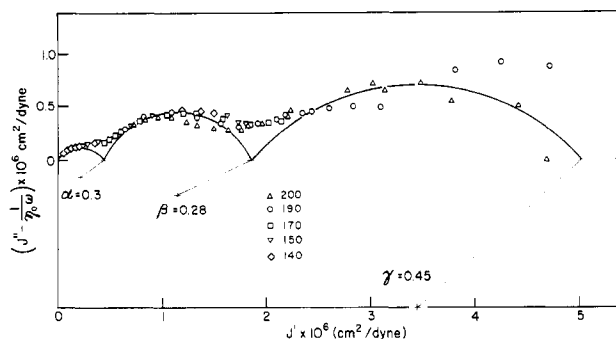


Figure 12. Cole-Cole plot for C732. The three arcs represent three retardation mechanisms. Symbols: (\diamond) data at 140.7; (∇) 150.4; (\square) 169.4; (\circ) 190.0; (Δ) 199.1 $^{\circ}\text{C}$.

mated visually as indicated by the small arrows in Figures 10 and 11. They are given in Table IV. Values were also obtained by fitting the data to an analytical expression. The complex dynamic compliance can be written as

$$J^*(\omega) = J_g + 1/j\omega\eta_0 + J_r^*(\omega) \quad (17)$$

where J_g is the glassy compliance (10^{-10} cm^2/dyn and therefore negligibly small relative to the other terms) and $J_r^*(\omega)$ is the complex retardational compliance. $J_r^*(\omega)$ is considered to be a sum of dispersions which are represented by a Cole-Cole equation²⁹

$$J_r^*(\omega) = \sum_n \frac{J_n}{1 + (j\omega\tau_n)^{1-\alpha_n}} \quad (18)$$

where J_n , τ_n , and α_n are empirical constants for each dispersion. For linear polymers $n = 2$. A Cole-Cole plot ($J_r''(\omega)$ vs. $J_r'(\omega)$) is shown for the C732 comb in Figure 12. Three circular arcs are drawn through the data indicating that $n = 3$ for comb polymers. The arc on the left represents the transition region and is given by one term of eq 18 with $J_r = 4.5 \times 10^{-7}$ cm^2/dyn , $\tau_r = 6.3 \times 10^{-4}$ s, and $\alpha_r = 0.3$. These values are identical with those determined for linear and star polystyrene melts.^{9,28} Likewise J_{br} , τ_{br} , and α_{br} were obtained from the intermediate arc and J_{bb} , τ_{bb} , and α_{bb} from the arc on the right. Values for all samples are given in Table IV. Resolution becomes difficult when the dispersions begin to overlap and substantial uncertainty is expected in the constants.

The values of τ_{br} and τ_{bb} obtained by the two methods are in fair agreement when the peaks are well separated but can differ substantially when the peaks merge (cf. C612 and C652).

In Figure 13 τ_{br} and τ_{bb} are plotted as a function of branch molecular weight. In each comb series τ_{bb} rises rapidly from the value for the parent backbone but the rate of increase becomes less at higher branch lengths than that for τ_{br} . In the case of the C6 series τ_{br} and τ_{bb} become similar in magnitude for the C652 sample. In the case of the C7 series the ratio of branch to backbone molecular weight is smaller and the spacing between τ_{br} and τ_{bb} is larger than in the C6 series.

The values of τ_{br} appear in Figure 13 to be roughly an exponential function of M_{br} over the experimental range

$$\log \tau_{br} \propto M_{br} \quad (19)$$

Such a dependence is predicted for the configurational renewal time of an entangled chain which is anchored at one end.¹⁴ On the other hand, Figure 14 is a double-logarithmic plot of the same data, suggesting

$$\tau_{br} \propto M_{br}^3 \quad (20)$$

Such a dependence would be expected for chains which renew their configurations by simple reptation.¹¹ It is

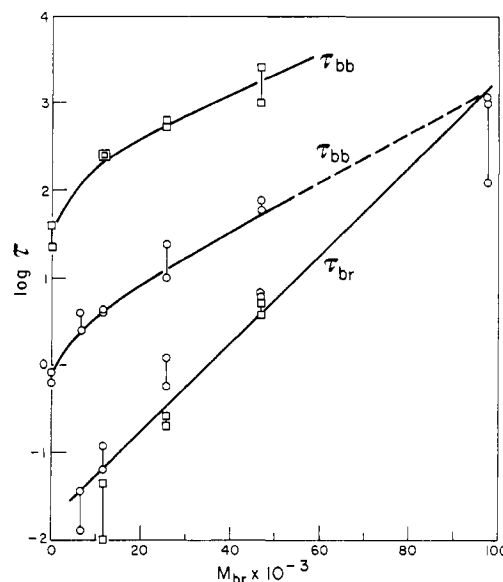


Figure 13. Characteristic retardation times vs. the molecular weight of the branches according to eq 19. Symbols: (\circ) C6 series; (\square) C7 series. All data at 169.5 $^{\circ}\text{C}$.

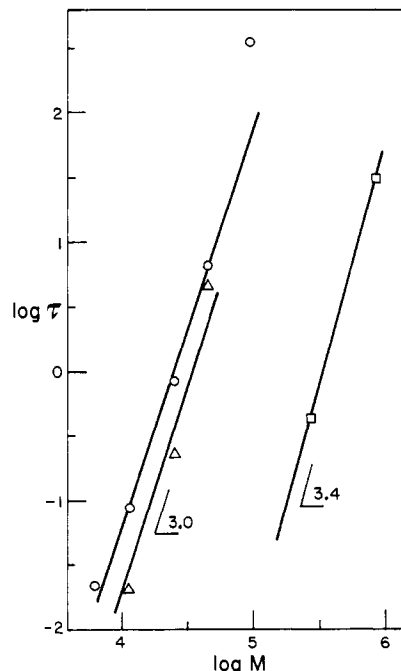


Figure 14. Characteristic retardation times vs. molecular weight according to eq 20. $\tau = \tau_{br}$, $M = M_{br}$ for the comb polymers. τ represents the terminal characteristic time for the linear polymers. Symbols: (\circ) C6 series; (Δ) C7 series; (\square) linear polymers.

therefore obvious that with the rather large errors expected in τ_{br} and the limited molecular weights of the branches ($(6-98) \times 10^3$) the present results do not permit a definite conclusion in favor of either mechanism. Curvatures of the τ_{br} plots in Figures 13 and 14 may reflect a transition from reptation at low M_{br} to anchored chain behavior at high M_{br} .

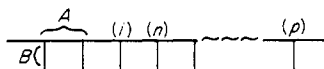
The values of τ_{br} for the C7 combs are somewhat smaller than the C6 combs with the same branch length. In view of the large uncertainty in the values of τ it is perhaps premature to speculate on this phenomenon, but the larger branch spacing in the C7 series ($860000/30 = 29000$) compared to the C6 series ($275000/30 = 9000$) may provide greater possibility for local cooperation between backbone and branches.

From Figure 14 it can be seen that the retardation times associated with the branches are orders of magnitude larger than those of free polystyrene chains of the same molecular weight. This is reminiscent of the slow processes attributed to dangling ends in networks³⁰ and block copolymers.³¹

Acknowledgment. We are grateful to W. Rochefort, V. Raju, and E. Menezes for help with various parts of this work. Use of the facilities of the Northwestern University Materials Research Center, supported by the National Science Foundation (Grant DMR 76-80847), is acknowledged with gratitude.

Appendix

A monodisperse backbone with p equidistantly placed monodisperse branches is considered as shown:



The number of branches = p , $A = M_{bb}/(p + 1)$, and $B = M_{br}$.

1. Starting from one end of the backbone

$$M_{EE'} = (p + 1)A + \sum_{i=1}^{p-1} (iA + B) \\ = \frac{(p + 1)(p + 2)}{2} A + pB$$

The total for the two backbone ends is

$$2M_{EE'} = (p + 1)(p + 2)A + 2pB \quad (1')$$

and the number of end-to-end combinations is $2(p + 1)$.

2. Starting from the end of the n th branch

$$M_{EE''} = (B + nA) + \sum_{i=1}^{n-1} (iA + 2B) + \\ (B + (p - n + 1)A) + \sum_{i=1}^{p-n} (iA + 2B) \\ = 2pB + n^2A + (p + 1)[p/2 - n + 1]A$$

which summed over all branches n from 1 to p is

$$pM_{EE''} = 2p^2B + \frac{p(p + 1)(p + 2)}{3} A \quad (2')$$

and the number of end-to-end combinations starting from

a branch end is $p(p + 1)$. \bar{M}_{EE} is the sum of all molecular weights between each two ends of the comb $(1') + (2')$ divided by the total number of end-to-end combinations and is given by eq 10. For $p \gg 3$, eq 10 reduces to

$$\bar{M}_{EE} = 2M_{br} + M_{bb}/3$$

which for a star with many branches becomes $\bar{M}_{EE} = 2M_{br}$.

References and Notes

- (1) See, e.g.: Rokudai, M. *J. Appl. Polym. Sci.* **1979**, *23*, 463.
- (2) Berry, G. C.; Fox, T. G. *Adv. Polym. Sci.* **1968**, *5*, 261.
- (3) Kraus, G.; Gruver, J. T. *J. Polym. Sci., Part A* **1965**, *3*, 105.
- (4) Meyer, H. H.; Ring, W. *Kautsch. Gummi Kunstst.* **1971**, *24*, 526.
- (5) Masuda, T.; Ohta, Y.; Onogi, S. *Macromolecules* **1971**, *4*, 763.
- (6) Utracki, L. A.; Roovers, J. *Macromolecules* **1973**, *6*, 366, 371.
- (7) Roovers, J.; Hadjichristidis, N. *J. Polym. Sci., Polym. Phys. Ed.* **1974**, *12*, 2521.
- (8) Graessley, W. W.; Masuda, T.; Roovers, J.; Hadjichristidis, N. *Macromolecules* **1976**, *9*, 127.
- (9) Graessley, W. W.; Roovers, J. *Macromolecules* **1979**, *12*, 959.
- (10) Graessley, W. W. *Adv. Polym. Sci.* **1974**, *16*, 1.
- (11) Doi, M.; Edwards, S. F. *J. Chem. Soc., Faraday Trans. 2* **1978**, *74*, 1802. See also: de Gennes, P. G. *J. Chem. Phys.* **1971**, *55*, 572.
- (12) Bueche, F. *J. Chem. Phys.* **1964**, *40*, 484.
- (13) Ham, J. S. *J. Chem. Phys.* **1957**, *26*, 625.
- (14) de Gennes, P. G. *J. Phys. (Paris)* **1975**, *36*, 1199.
- (15) Fujimoto, T.; Narukawa, H.; Nagasawa, M. *Macromolecules* **1970**, *3*, 57.
- (16) Noda, I.; Horikawa, T.; Kato, T.; Fujimoto, T.; Nagasawa, M. *Macromolecules* **1970**, *3*, 795.
- (17) Fujimoto, T.; Kajiura, H.; Hirose, M.; Nagasawa, M. *Polym. J.* **1972**, *3*, 181.
- (18) Pannell, J. *Polymer* **1972**, *13*, 1.
- (19) Roovers, J. *Polymer* **1975**, *16*, 827.
- (20) Roovers, J. *Polymer* **1979**, *20*, 843.
- (21) Long, V. C.; Berry, G. C.; Hobbs, L. M. *Polymer* **1964**, *5*, 517.
- (22) Graessley, W. W.; Shinbach, E. S. *J. Polym. Sci., Polym. Phys. Ed.* **1974**, *12*, 2047.
- (23) Ferry, J. D. "Viscoelastic Properties of Polymers", 2nd ed.; Wiley: New York, 1970.
- (24) Macosko, C. W.; Davis, W. M. *Rheol. Acta* **1974**, *13*, 814.
- (25) Casassa, E. F.; Berry, G. C. *J. Polym. Sci., Part A-2* **1966**, *4*, 881.
- (26) Pannell, J. *Polymer* **1971**, *12*, 558.
- (27) Candau, F.; Rempp, P.; Benoit, H. *Macromolecules* **1972**, *5*, 627.
- (28) Pearson, D.; Raju, V., private communication.
- (29) Marin, G.; Graessley, W. W. *Rheol. Acta* **1977**, *16*, 527.
- (30) Langley, N. R.; Ferry, J. D. *Macromolecules* **1968**, *1*, 353.
- (31) Cohen, R. E.; Tschögl, N. W. *Int. J. Polym. Mater.* **1973**, *2*, 205.

Solubility Behavior of Copolymers of Isoprene and Sodium Styrenesulfonate

B. Siadat,* R. D. Lundberg,[†] and R. W. Lenz

Materials Research Laboratory, Chemical Engineering Department, University of Massachusetts, Amherst, Massachusetts 01003. Received October 10, 1980

ABSTRACT: Solubility studies were made on poly(isoprene-co-sodium styrenesulfonate) ionomers in nonpolar hydrocarbon solvents and in mixed solvents containing a minor amount of alcohol. It was shown that these isoprene-based ionomers were ionically aggregated and that alcohols effectively solvated the ionic associations. The temperature dependence of the solution viscosity of these ionomers was also investigated.

Introduction

Modification of partially unsaturated elastomeric hydrocarbon polymers by sulfonation has been recently re-

ported by several investigators.¹⁻⁴ The rheological and tensile properties⁵ of these sulfonated elastomers as well as their thermal and dynamic mechanical responses³ have been characterized and disclosed. We have been able to extend the scope of these ion-containing elastomers by successfully copolymerizing diene monomers with a number of olefinic sulfonic acid salts.⁶

Evidence shown in recent studies^{3,7} indicates that pen-

* To whom correspondence should be addressed at W. R. Grace & Co., Research Division, Columbia, MD 21044.

[†] Present address: Corporate Research—Science Laboratory, Exxon Research and Engineering Company, Linden, NJ 07036.